11th World Congress on Computational Mechanics (WCCM XI)
5th European Conference on Computational Mechanics (ECCM V)
6th European Conference on Computational Fluid Dynamics (ECFD VI)
E. Oñate, J. Oliver and A. Huerta (Eds)

FREESTREAM PRESERVATION ON A HIGH-ORDER CONSERVATIVE FR SCHEME

Yoshiaki Abe[1], Takanori Haga[2], Taku Nonomura[3], and Kozo Fujii[3]

[1] University of Tokyo, Sagamihara, 2525210, Japan, Email: abe@flab.isas.jaxa.jp
[2] JAXA's Engineering Digital Innovation Center, JAXA, Sagamihara, 2525210, Japan
Email: haga.takanori@jaxa.jp
[3] Institute of Space and Astronautical Science, JAXA, Sagamihara, 2525210, Japan
Email: nonomura, fujii@flab.isas.jaxa.jp

Key words: high-order flux reconstraction scheme, complex geometries, geometric conservation law, body-fitted coordinate, freestream preservation.

Abstract. The appropriate procedure for constructing symmetric conservative metrics is presented with which both of the freestream preservation and global conservation properties are satisfied in the high-order conservative flux-reconstruction scheme on a three-dimensional stationary-curvilinear grid. A freestream preservation test is conducted, and the symmetric conservative metrics constructed by the appropriate procedure preserve the freestream with regardless of the order of shape functions, while other metrics cannot always preserve the freestream. Also a convecting vortex is computed on three-dimensional wavy grids, and the formal order of accuracy is achieved when the symmetric conservative metrics are appropriately constructed, while it is not when they are inappropriately constructed.

1 Introduction

Recently, various methods with high-order spatial accuracy have been developed on unstructured grids, e.g., discontinuous Galerkin (DG), spectral difference (SD), spectral volume (SV), and flux reconstruction (FR) schemes [1][2]. The present study focuses on the FR scheme [1], which computes with an accuracy similar to that of the DG scheme, but with reduced computational cost. Specifically, the study investigates the conservative FR scheme [2], in which the governing equation is expressed in a strong conservation form.

When computing flows around complex geometries using conventional high-order finite-difference schemes, the generalized (body-fitted) coordinate system is frequently adopted. In this construct, the fidelity of the represented boundary shape directly depends on the number of grid points. In contrast, in the FR scheme, the boundary shape of each cell is analytically defined by a high-order shape function. Consequently, the number of computational grid points, which should be predetermined, is significantly reduced. Such a

vast reduction of grid points also alleviate some of the difficulties in generating grids with complicated geometries. However, despite the strong conservation form of the governing equation, the use of the generalized coordinate system and high-order shape functions often fails to compatibly satisfy both of the freestream preservation [3] and global conservation [4][5] properties [1]. A versatile technique [6][7][8][9][10][4][5][11] has been introduced for high-order finite-difference schemes, in which a metric is analytically re-expressed in conservative form. The use of conservative metrics is similarly expected to ensure both of the freestream preservation and global conservation properties in the FR scheme, but the implementation is not straightforward. In a study of the discontinuous spectral element (DSE) scheme, Kopriva [3] demonstrated that if the order of the solution is less than twice of the order of the shape function, then freestream is not preserved with nonconservative (cross product form) metrics. Kopriva also proposed a scheme that satisfies freestream preservation through applying conservative metrics. However, the following items are still unclear: 1) The conditions required for compatibly satisfying both of the freestream preservation and global conservation properties; 2) Detailed procedures for constructing conservative metrics which satisfy the freestream preservation property; 3) The accuracy of numerical solutions based on conservative metrics. Therefore, in this paper, the following items are newly summarized for the FR scheme: 1) Compatible conditions required for satisfying both of the freestream preservation and global conservation properties are presented (Sec. 2.3 and Sec. 3); 2) Detailed procedures are established for constructing conservative metrics which satisfy the freestream preservation property without neglecting the global conservation property (Sec. 4); 3) The order of accuracy of the numerical solutions based on the conservative metrics is evaluated (Sec. 5).

2 Conservative flux-reconstruction scheme

2.1 Coordinate system and inner degrees of freedom

The computational domain is subdivided into hexahedral cells. Each hexahedral cell in the Cartesian coordinate system $\{x, y, z\}$ of physical space is mapped onto a standard cube cell $E_s := \{\xi, \eta, \zeta | -1 \leq \xi, \eta, \zeta \leq 1\}$ in the generalized coordinate system $\{\xi, \eta, \zeta\}$ of computational space. Figure 1 shows one cell in the case of $N = 1$. The GP is defined at the cell vertex (the blue points in Fig. 1). In this study, the Gauss point is applied to SP.

2.2 Discretization of the governing equations

In the following, the indices i, j, and k indicate GPs, and p, q, and r indicate SPs (Gauss points). The shape of the nth cell is approximated by the tensor product:

$$\boldsymbol{r}_n^{GP;N}(\xi, \eta, \zeta) := I^{GP;N}[\boldsymbol{r}_n] = \sum_{i,j,k=0}^{N} M_{n;i}^N(\xi) M_{n;j}^N(\eta) M_{n;k}^N(\zeta) \boldsymbol{r}_{n;i,j,k}, \tag{1}$$

[1] The global conservation property is called "integrated conservation property" in [4][5].

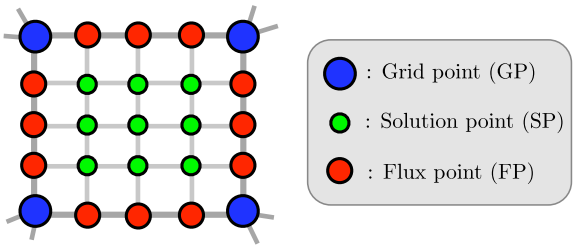

Fig. 1: Schematic of grid, solution and flux points in each cell. The orders of the shape function and solution polynomial are $N = 1$ and $K = 2$, respectively.

where $M^N_{n;i}(\xi)$, $M^N_{n;j}(\eta)$, and $M^N_{n;k}(\zeta)$ are the shape functions for GP at (ξ_i, η_j, ζ_k). The Jacobian for coordinate transformation is $J := |\partial(x, y, z)/\partial(\xi, \eta, \zeta)|$, and the metrics (e.g., $\hat{\xi}_x := \xi_x J$) are defined [2] as follows:

$$\hat{\xi}_x = y_\eta z_\zeta - z_\eta y_\zeta, \quad J = x_\xi y_\eta z_\zeta - x_\eta y_\xi z_\zeta + x_\zeta y_\xi z_\eta - x_\xi y_\zeta z_\eta + x_\eta y_\zeta z_\xi - x_\zeta y_\eta z_\xi, \tag{2}$$

Hereafter, each analytical form in Eq.(2) is called a nonconservative form (NC). The compressible Euler equations in the generalized coordinate system are

$$\partial_\tau \hat{Q} + \partial_\xi \hat{E} + \partial_\eta \hat{F} + \partial_\zeta \hat{G} = 0, \tag{3}$$

To solve the governing equation (3), the spatial distribution of the conservative quantity in the nth cell, Q_n, is approximated by the tensor product for the Kth-order Lagrange polynomial interpolation using $(K+1)^3$ discrete values of Q_n at SPs. The present approximation of Q_n is denoted as $Q^{SP;K}_n := I^{SP;K}[Q_n]$. Specifically, we have

$$Q^{SP;K}_n := I^{SP;K}[Q_n] = \sum_{p,q,r=0}^{K} \phi^K_{n;p}(\xi)\phi^K_{n;q}(\eta)\phi^K_{n;r}(\zeta) Q_{n;p,q,r}, \tag{4}$$

where $\phi^K_{n;p}$ is the Kth-order Lagrange polynomial. When the Kth-order polynomial interpolation is employed, a spatial $(K+1)$th-order scheme is formulated.

Next, we explain the procedure for the computation of flux divergence at each SP. Without loss of generality, we consider only the differential in the ξ-direction of $\hat{E}$ in the nth cell, keeping the other coordinates fixed ($\eta = \eta_q, \zeta = \zeta_r$). Using the discrete values of $Q^{SP;K}_n$ at SP, the nth cell inner distributions $\hat{E}^{SP}_n$ and $\partial_\xi \hat{E}^{SP}_n$ are expressed by a Kth-order polynomial interpolation as follows:

$$\hat{E}^{SP;K}_n(\xi) = I^{SP;K}[\hat{E}^{SP}_n](\xi) \equiv \sum_{p=0}^{K} \phi^K_{n;p}(\xi)\hat{E}^{SP}_{n;p,q,r}. \tag{5}$$

[2] In this paper, the partial derivative of a physical quantity f in the x-direction is denoted $\partial_x f$ or f_x; both notations are used interchangeably.

Since this flux is constructed without information from the adjacent cells, $\hat{E}_n^{SP;K}$ is discontinuously distributed. Therefore, the reconstructed flux $\hat{E}_n^C$ is defined to be continuous at the cell boundaries. First, a flux point (hereafter "FP": red points in Fig. 1) is placed at the intersection of the planes surrounding the cell and lines passing through SPs in each direction at the cell boundaries. Next, the solutions of Q^L and Q^R at FPs on both sides of the boundaries are extrapolated using Eq.(4), and $\hat{E}^{com}$ is determined by an approximate Riemann solver. Finally, the original Kth-order flux $\hat{E}_n^{SP;K}$ is modified such that $\hat{E}_n^C$ equals $\hat{E}^{com}$ at FP:

$$\hat{E}_n^C(\xi) = \hat{E}_n^{SP;K}(\xi) + \left[\hat{E}_{n-1/2}^{com} - \hat{E}_n^{SP;K}(-1)\right] g_L(\xi) + \left[\hat{E}_{n+1/2}^{com} - \hat{E}_n^{SP;K}(+1)\right] g_R(\xi). \quad (6)$$

Here, the subscripts $n \mp 1/2$ indicate the left and right boundaries, respectively, of the nth cell. $g_L(\xi)$ is a $(K+1)$th-order polynomial in which the left and right boundaries ($\xi = -1$ and $\xi = +1$, respectively) are valued at 1 and 0, respectively. g_R is the symmetric function of g_L about the origin ($g_R(\xi) = -g_L(-\xi)$).

2.3 Global conservation property

The global conservation property specifies that the integration of conservative quantities over the computational region is conserved [4]. Even if the strong conservation form is adopted in the governing equation, the global conservation property is violated if the discretization is inappropriate. First, we discuss the conservation property within individual cells Ω_n (the local conservation property). Within the nth cell, the local conservation property holds if the following equation is satisfied:

$$\int_{\Omega_n} \partial_\xi \hat{E}_n^C d\xi = \hat{E}_{n+1/2}^{com} - \hat{E}_{n-1/2}^{com}, \quad (7)$$

where Ω_n indicates the closed domain in the nth cell. The flux $\hat{E}_n^C$ obtained in Eq.(6) is the continuous Kth-order polynomial found within the cells containing boundaries and satisfies Eq.(7). Because SPs are Gauss points, $\hat{E}_n^{SP;K}(\pm 1)$ in Eq.(6) is extrapolated from $\hat{E}_n^{SP;K}$ in Eq.(5). In such cases, the flux must be computed after extrapolating the conservative quantity Q_n to avoid nonconformities introduced by the polynomial interpolation approximation. Next, we discuss the conservation property within the computational domain V (the global conservation property). If the local conservation property holds within each cell Ω_n, as a sufficient condition for the global conservation property, the following equation must be satisfied within an arbitrary closed domain ${}^\forall\Omega \subset V$:

$$\sum_{n \in {}^\forall\Omega} \int_{\Omega_n} \partial_\xi \hat{E}_n^C d\xi = \sum_{n \in {}^\forall\Omega} (\hat{E}_{n+1/2}^{com} - \hat{E}_{n-1/2}^{com}) = \hat{E}_{n_{\max \text{ of } {}^\forall\Omega}+1/2}^{com} - \hat{E}_{n_{\min \text{ of } {}^\forall\Omega}-1/2}^{com}, \quad (8)$$

where $(n_{\max \text{ of } {}^\forall\Omega} + 1/2)$ and $(n_{\min \text{ of } {}^\forall\Omega} - 1/2)$ indicate the upper and lower boundary of the closed domain ${}^\forall\Omega$, respectively. Regarding $\hat{E}_{n\pm1/2}^{com}$ at each cell boundary (at FP), if

the adjacent cells share a common value, the total sum in the left-hand side of Eq. (8) is the boundary integral of the closed domain ${}^{\forall}\Omega$. Therefore, Eq.(8) is numerically satisfied by uniquely determining $\hat{E}^{com}_{n\pm1/2}$ on each cell boundary (at FPs), and thereby gives a sufficient condition for the global conservation property.

If the grid is shaped by curved lines, the metrics used in $\hat{E}^{com}_{n\pm1/2}$ may not be uniquely determined at the boundaries between adjacent cells, and the condition is violated. Therefore, we obtain the appropriate evaluation method for metrics, inspired by the previously proposed methods on characteristic interface conditions formulated in finite-difference schemes [12]. In our method, the metrics are constructed by interpolating common discrete values found in each adjacent cell. In this study, all metrics will be constructed to guarantee the global conservation property. Compatible combination of the concepts for freestream preservation and global conservation properties requires special ingenuity, since the freestream preservation property is independently (locally) treated in each cell whereas the global conservation property considers the values of adjacent cells.

3 Conditions for freestream preservation in the FR scheme

Although the freestream preservation property is often violated in finite-difference schemes, it has not been adequately discussed in either the DG or FR schemes [3] when the cells are expressed by high-order shape functions. In this section, we organize and collate all sufficient conditions for freestream preservation in the FR scheme. In the following, we discuss the interior of the nth cell (partially abbreviating the subscripted n values). The conditions for freestream preservation at SPs are reduced to the surface closure law (SCL identities) [4][5] given by

$$\partial_\xi \hat{\xi}^C_x + \partial_\eta \hat{\eta}^C_x + \partial_\zeta \hat{\zeta}^C_x = 0, \quad \partial_\xi \hat{\xi}^C_y + \partial_\eta \hat{\eta}^C_y + \partial_\zeta \hat{\zeta}^C_y = 0, \quad \partial_\xi \hat{\xi}^C_z + \partial_\eta \hat{\eta}^C_z + \partial_\zeta \hat{\zeta}^C_z = 0. \tag{9}$$

The metric $\hat{\xi}^C_x = \{\xi_x J\}^C$ is hereafter referred to as the "reconstructed metric". Adhering to Eq.(6), $\hat{\xi}^C_x$ is written as

$$\hat{\xi}^C_x(\xi) = \hat{\xi}^{SP}_x(\xi) + \left[\hat{\xi}^{GP}_x(-1) - \hat{\xi}^{SP}_x(-1)\right] g_L(\xi) + \left[\hat{\xi}^{GP}_x(+1) - \hat{\xi}^{SP}_x(+1)\right] g_R(\xi). \tag{10}$$

Here, $\hat{\xi}^{SP}_x$ and $\hat{\xi}^{GP}_x$ are the interpolating polynomials constructed from the discrete metric values at SPs and GPs, respectively. The ±1 argument indicates FP at the left and right sides of each cell. It should be noted that if the metric in FP is not set to $\hat{\xi}^{GP}_x(\pm1)$ and if the equation is not constructed to search for common values in the shared FPs among adjacent cells, the global conservation property will deteriorate. Rewriting the left-hand side of SCL identity (Eq.(9)) by the expression of Eq.(10), we obtain

$$\text{Left-hand side of Eq.(9)} \iff \underbrace{\partial_\xi \hat{\xi}^{SP}_x + \partial_\eta \hat{\eta}^{SP}_x + \partial_\zeta \hat{\zeta}^{SP}_x}_{\text{SP part}} + \underbrace{\left[\hat{\xi}^{GP}_x(-1) - \hat{\xi}^{SP}_x(-1)\right] dg_L(\xi)/d\xi + \ldots}_{\text{correction part}}. \tag{11}$$

The conditions under which both underlined terms (SP and correction parts) in Eq.(11) equal 0 at SPs are summarized bellow. When computing the metric, if any of the conditions described below are satisfied, then SP part becomes zero at SP:

Sufficient conditions for SP part being equal to 0

(A-1) The nonconservative metric is used while the order of the solution polynomial is equal to or greater than twice of the order of the shape function.

or

(A-2) The symmetric conservative metric is used (the order of the solution polynomial is greater than that of metrics, as shown in Appendix A).

If condition (A-1) is satisfied, the value of $\partial_\xi \hat{\xi}_x^{SP}(\xi)$ computed by NC corresponds to the analytical value defined by the shape function, and SP part becomes zero. In contrast, the symmetric conservative metrics (SC) as specified in condition (A-2) are expressed in terms of T_A, T_B, and T_C as shown below:

$$\hat{\xi}_x = \{(y_\eta z - z_\eta y)_\zeta - (y_\zeta z - z_\zeta y)_\eta\}/2 = T_{A\zeta} - T_{B\eta}, \hat{\eta}_x = T_{B\xi} - T_{C\zeta}, \hat{\zeta}_x = T_{C\eta} - T_{A\xi}. \quad (12)$$

Although these equations are analytically equivalent to the nonconservative metric given by Eq.(2), they generally differ when discretized in the computation. If the symmetric conservative metric is used, SP part becomes zero under the conditions defined in Appendix A because the interpolation and differentials are commutative.

When computing the metrics, the following condition ensures that the correction part in Eq.(11) becomes zero:

Sufficient condition for correction part being equal to 0

(B) $\hat{\xi}_x^{GP}(\pm 1) = \hat{\xi}_x^{SP}(\pm 1)$, $\hat{\eta}_x^{GP}(\pm 1) = \hat{\eta}_x^{SP}(\pm 1)$, and $\hat{\zeta}_x^{GP}(\pm 1) = \hat{\zeta}_x^{SP}(\pm 1)$.

When conditions A are met for the SP part, condition (B) is concurrently satisfied in our framework locating some of GP at the cell boundaries (see Sec. 2.3).

4 Computational procedure for constructing the metrics

This section details the procedures for implementing all three forms of the metrics (the nonconservative (NC), symmetric conservative (SC), and high-order symmetric-conservative metric (SCHGP)).

4.1 Nonconservative metric (NC)

NC is the typical form of a metric. It is described by Eq.(2) and computed by the following procedure.

Step 1:**Nth-order interpolating polynomial** y

Define the Nth-order interpolating polynomial for y (and similarly for z) based on the discrete values at GPs using the Nth-order shape functions as follows:

$$I^{GP;N}[y] = \sum_{i,j,k=0}^{N} M_i^N(\xi) M_j^N(\eta) M_k^N(\zeta) y_{i,j,k}, \tag{13}$$

Step 2:**Nth-order interpolating polynomial** y_n

Compute the Nth-order interpolating polynomial for y_η (and similarly for another differential) using the Nth-order shape function and the coordinate values at GPs:

$$\partial_\eta I^{GP;N}[y] = \sum_{i,j,k=0}^{N} M_i^N(\xi) dM_j^N(\eta) M_k^N(\zeta) y_{i,j,k}, \tag{14}$$

where $dM_j^N(\xi) := dM_j^N/d\xi$ denotes differentiation of $M_j^N(\xi)$ with respect to ξ.

Step 3: **$2N$th-order interpolating polynomial** $\hat{\xi}_x^{GP;2N}$

Compute the $2N$th-order interpolating polynomial for $\hat{\xi}_x$ as follows:

$$\hat{\xi}_x^{GP;2N} = \partial_\eta I^{GP;N}[y] \partial_\zeta I^{GP;N}[z] - \partial_\zeta I^{GP;N}[y] \partial_\eta I^{GP;N}[z]. \tag{15}$$

Since this polynomial matches the metric of the exact grid shape (which is analytically defined by the Nth-order shape function), $\hat{\xi}_x^{GP;2N}$ is hereafter referred to as the true metric.

Step 4: **Kth-order interpolating polynomial** $\hat{\xi}_x^{SP;K}$

Reconstruct the Kth-order interpolating polynomial for $\hat{\xi}_x$ from the discrete values at SP of the $\hat{\xi}_x^{GP;2N}$ given by Eq.(15):

$$\hat{\xi}_x^{SP;K} = I^{SP;K}[\hat{\xi}_x^{GP;2N}] = \sum_{p,q,r=0}^{K} \phi_p^K(\xi) \phi_q^K(\eta) \phi_r^K(\zeta) \hat{\xi}_{x;p,q,r}^{GP;2N}. \tag{16}$$

The reconstructed metric $\hat{\xi}_x^C$ given by Eq.(10) is computed from $\hat{\xi}_x^{SP;K}$ and $\hat{\xi}_x^{GP;2N}$, which respectively replace $\hat{\xi}_x^{SP}$ and $\hat{\xi}_x^{GP}$ in Eq.(10). When $K \geq 2N$, $\hat{\xi}_x^{SP;K}$ is the true metric $\hat{\xi}_x^{GP;2N}$ [3]. The interpolation from $\hat{\xi}_x^{GP;2N}$ to $\hat{\xi}_x^{SP;K}$ in *Step 4* may introduce truncation

[3]Although $\hat{\xi}_x^{SP;K} = \hat{\xi}_x^{GP;2N}$ holds at SP, it does not hold elsewhere (see Appendix A). Therefore, $\partial_\xi \hat{\xi}_x^{SP;K} \neq \partial_\xi \hat{\xi}_x^{GP;2N}$, and each item in the SCL identity is not analytically matched.

and aliasing errors when $K < 2N$. Therefore, when the NC is used for metrics, the SCL identity is satisfied only when $K \geq 2N$. Consequently, the implementation of NC for the freestream preservation becomes increasingly difficult as the order of the shape function increases. For example, when the order of the shape function N is 2, the order of the solution K must be 4. Additionally, when grids are moving and deforming, the metric computation involves three-dimensional nonlinear terms (for example, $x_t y_\zeta z_\eta$), requiring an additional strict condition $K \geq 2N + N_t$ (here, N and N_t denote the order of the shape function in the spatial and temporal directions, respectively).

4.2 Symmetric conservative metric (SC)

When SC is applied, since the differential used in the construction of T_A and T_B given by Eq.(12) commutes with the differential in the flux divergence, the SCL identity given by Eq.(9) is satisfied in the absence of a true metric given by Eq.(15). Therefore, the acceptable range of the order of solution broadens from $K \geq 2N$ to $K \geq N$ (see Appendix A). *Step 1* and *Step 2* in the construction of SC are identical to *Step 1* and *Step 2* of NC, and are hence omitted.

Step 3: $2N$**th-order interpolating polynomial** $T_A^{GP;2N}, T_B^{GP;2N}$

Compute the $2N$th-order interpolating polynomials T_A (and similarly for T_B) using the Nth-order shape function and the coordinate values at GP:

$$2T_A^{GP;2N} = \partial_\eta I^{GP;N}[y] I^{GP;N}[z] - \partial_\eta I^{GP;N}[z] I^{GP;N}[y]. \tag{17}$$

Step 4: N**th-order interpolating polynomial** $\hat{\xi}_x^{GP;N}$

Define the interpolating polynomial $\hat{\xi}_x = T_{A\zeta} - T_{B\eta}$ using the Nth-order shape function:

$$\begin{aligned}\hat{\xi}_x^{GP;N} &= \partial_\zeta I^{GP;N}[T_A^{GP;2N}] - \partial_\eta I^{GP;N}[T_B^{GP;2N}] \\ &= \sum_{i,j,k=0}^{N} \left\{ M_i^N(\xi) M_j^N(\eta) dM_k^N(\zeta) T_{A;i,j,k}^{GP;2N} - M_i^N(\xi) dM_j^N(\eta) M_k^N(\zeta) T_{B;i,j,k}^{GP;2N} \right\}. \end{aligned} \tag{18}$$

Because $\hat{\xi}_x^{GP;N}$ in Eq.(18) is computed by an Nth-order interpolation using the discrete values T_A and T_B, $\hat{\xi}_x^{GP;N}$ always differs from the true metric $\hat{\xi}_x^{GP;2N}$.

Step5: K**th-order interpolating polynomial** $\hat{\xi}_x^{SP;K}$

Reconstruct the Kth-order interpolating polynomial from the discrete values of $\hat{\xi}_x^{GP;N}$ at SP:

$$\hat{\xi}_x^{SP;K} = I^{SP;K}[\hat{\xi}_x^{GP;N}] = \sum_{p,q,r=0}^{K} \phi_p^K(\xi) \phi_q^K(\eta) \phi_r^K(\zeta) \hat{\xi}_{x;p,q,r}^{GP;N}. \tag{19}$$

The reconstructed metric $\hat{\xi}_x^C$ given by Eq.(10) is computed from $\hat{\xi}_x^{SP;K}$ and $\hat{\xi}_x^{GP;N}$ which respectively replace $\hat{\xi}_x^{SP}$ and $\hat{\xi}_x^{GP}$ in Eq.(10). If $K < N$, because Kth-order $\hat{\xi}_x^{SP;K}$ is reconstructed using a lower-order interpolation of Nth-order $\hat{\xi}_x^{GP;N}$, error occurs in the reconstruction [4]. Moreover, even if the order of the solution K is sufficiently high ($K \geq 2N$), $\hat{\xi}_x^{SP;K}$ corresponds to $\hat{\xi}_x^{GP;N}$ but not to the true metric $\hat{\xi}_x^{GP;2N}$. Therefore, the obtainable order of accuracy in the computational solution is not expected to exceed that in the metric (see Sec. 5).

4.3 Symmetric-conservative high-order metric (SCHGP)

Our proposed symmetric-conservative high-order metric (SCHGP) overcomes the two defects in SC by conforming the metric constructed at GPs to the Kth-order of the solution. In the construction of SCHGP, *Step 1* and *Step 2* are identical to NC, and *Step 3* is identical to SC.

Step 4: **Kth-order interpolating polynomial $\hat{\xi}_x^{GP;K}$**

Define $\hat{\xi}_x = T_{A\zeta} - T_{B\eta}$ using a Kth-order interpolating polynomial. Here, hi, hj, and hk denote the $(K+1)^3$ points (hereafter referred to as "high-order grid point (HGP)"). The HGPs do not need correspond to SPs. However, the global conservation property must be considered, and in each direction, the HGP must be placed within the cell boundaries (indicated by triangles in Fig. 2). Therefore, HGPs are always positioned at GPs at cell vertex.

$$\begin{aligned}\hat{\xi}_x^{HGP;K} &= \partial_\zeta I^{HGP;K}[T_A^{GP;2N}] - \partial_\eta I^{HGP;K}[T_B^{GP;2N}] \\ &= \sum_{hi,hj,hk=0}^{K} \left\{ M_{hi}^K(\xi) M_{hj}^K(\eta) dM_{hk}^K(\zeta) T_{A;hi,hj,hk}^{GP;2N} - M_{hi}^K(\xi) dM_{hj}^K(\eta) M_{hk}^K(\zeta) T_{B;hi,hj,hk}^{GP;2N} \right\}. \quad (20)\end{aligned}$$

Because the computation of $\hat{\xi}_x^{HGP;K}$ in Eq.(20) involves a Kth-order interpolation using the discrete values T_A and T_B, $\hat{\xi}_x^{HGP;K}$ corresponds to the true metric $\hat{\xi}_x^{GP;2N}$ when $K \geq 2N$.

Step 5: **Kth-order interpolating polynomial $\hat{\xi}_x^{SP;K}$**

Reconstruct the Kth-order interpolating polynomial $\hat{\xi}_x$ from the discrete values of $\hat{\xi}_x^{HGP;K}$ at SP:

$$\hat{\xi}_x^{SP;K} = I^{SP;K}[\hat{\xi}_x^{HGP;K}] = \sum_{p,q,r=0}^{K} \phi_p^K(\xi)\phi_q^K(\eta)\phi_r^K(\zeta)\hat{\xi}_{x;p,q,r}^{HGP;K}. \quad (21)$$

[4] When $K < N$, because $\hat{\xi}_x^{GP;N} \neq \hat{\xi}_x^{SP;K}$ at all location with the exception of SP, the metric $\hat{\xi}_x^{SP;K}$ cannot be written in the forms as found in Eq.(18) or in Eq.(22) of Appendix A.

The reconstructed metric $\hat{\xi}_x^C$ given by Eq.(10) is computed from $\hat{\xi}_x^{SP;K}$ and $\hat{\xi}_x^{HGP;K}$ which respectively replace $\hat{\xi}_x^{SP}$ and $\hat{\xi}_x^{GP}$ in the original Eq.(10). Because $\hat{\xi}_x^{SP;K}$ in Eq.(21) is computed by a Kth-order interpolation using the discrete values of $\hat{\xi}_x^{HGP;K}$, the following equality always holds: $\hat{\xi}_x^{SP;K} = \hat{\xi}_x^{HGP;K}$. As shown in Appendix A, $\hat{\xi}_x^{SP;K}$ satisfies the SCL identities (SP part= 0), and $\hat{\xi}_x^{SP;K} = \hat{\xi}_x^{HGP;K}$ also holds at FPs as well (correction part= 0). The conditions under which the three metrics satisfy freestream preservation property are summarized in Table 1. Here, K and N specify the orders of the solution and shape function, respectively.

Table 1: Expected freestream preservation characteristics of the metrics (∘ indicates freestream preservation; • indicates violation of freestream preservation property)

Order of solution K	$K < N$	$N \leq K < 2N$	$2N \leq K$
NC	•	•	∘
SC	•	∘	∘
SCHGP	∘	∘	∘

5 Computational test

In this section, we perform computational tests for metrics in NC, SC, and SCHGP. We consider a compressible inviscid fluid assumed as an ideal gas with specific heat ratio $\gamma = 1.4$ (relative to air). The governing equation is Eq.(3), and three-dimensional wavy grids are used. The flow fields are assumed to be periodic. We first conduct the freestream preservation test, and obtain the result that the relationship between the metrics which preserve the freestream and the order of the solution polynomial exactly comply with those listed in Table 1 (not presented in this paper). Next, a convecting two-dimensional vortex [13] is examined. Computations are performed until the convecting vortex returns to its initial position. The pressure distribution on the plane at constant z is shown in Fig. 3. Comparing this figure with Table 1, we find that the vortex degrades when the freestream is not preserved, but is retained when freestream is preserved. In particular, when the solution order $K = 4$, the vortex is much better preserved in the SCHGPs and NCs than in the SCs. This result demonstrates that even if the freestream is preserved, the vortex degrades if the order of the metric is below that of the solution polynomial (see Sec. 4.2). The L_2-norm of the swirl velocity v is shown in Fig. 4. Solutions do not properly converge when the freestream preservation is violated (see Fig. 4(a): $p1$–$p3$ for NC, Fig. 4(b): $p1$ for SC). In contrast, SCHGP shows increasingly improved convergence at higher orders. On the other hand, as in Sec. 4.2, even if the order of the solution is sufficiently high ($K > 2$), the order of the SC metrics cannot exceed the order of the shape function ($N = 2$). That is, regardless of the order of numerical solutions, convergence in SC cannot be improved beyond that of $p2$ in Fig. 4(b). Therefore, when the metrics are evaluated by SC, the order of the numerical solution is strictly limited by the order of metrics.

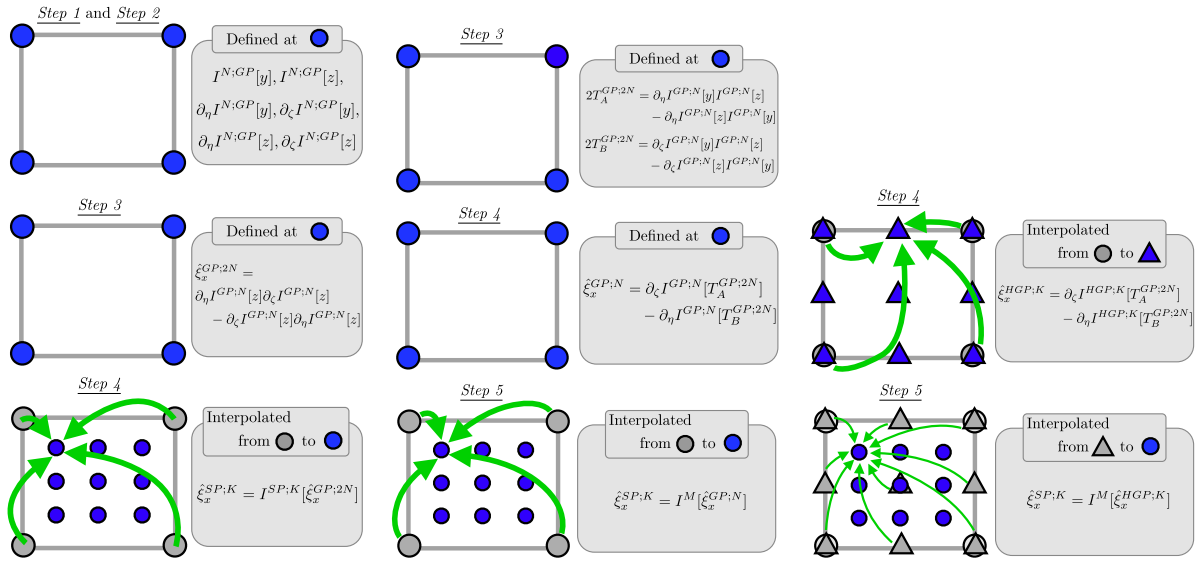

(a) NC (b) SC (c) SCHGP

Fig. 2: Schematic of NC, SC, and SCHGP metric with $N = 1$ and $K = 2$.

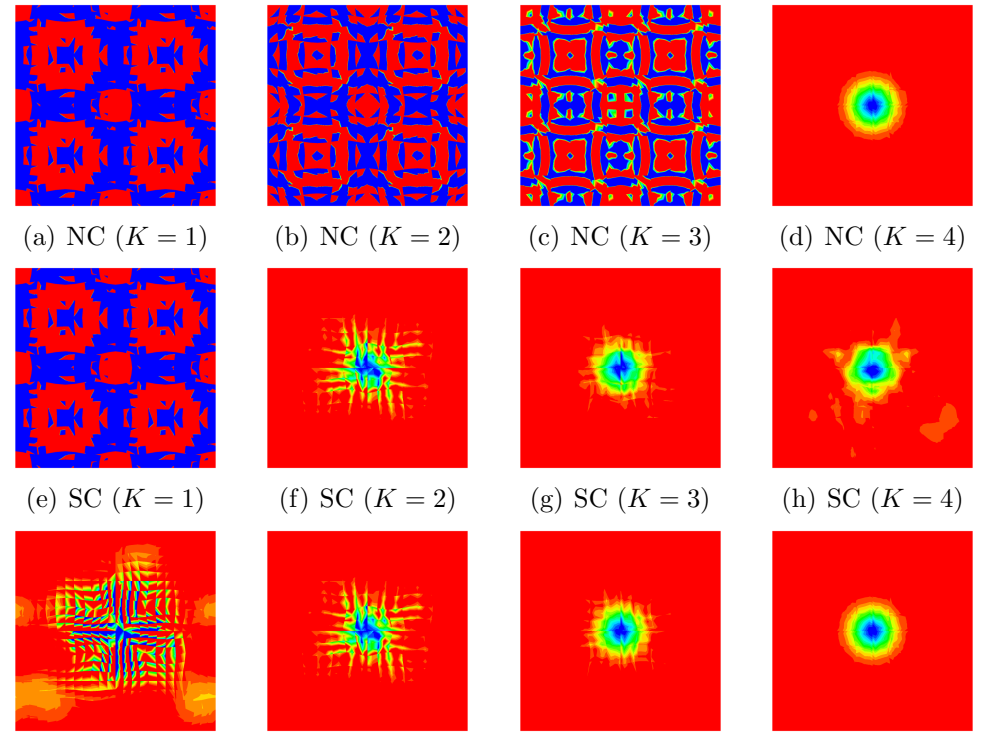

(a) NC ($K = 1$) (b) NC ($K = 2$) (c) NC ($K = 3$) (d) NC ($K = 4$)

(e) SC ($K = 1$) (f) SC ($K = 2$) (g) SC ($K = 3$) (h) SC ($K = 4$)

(i) SCHGP($K = 1$) (j) SCHGP($K = 2$) (k) SCHGP($K = 3$) (l) SCHGP($K = 4$)

Fig. 3: Contours of pressure distribution on a horizontal (z-constant) plane.

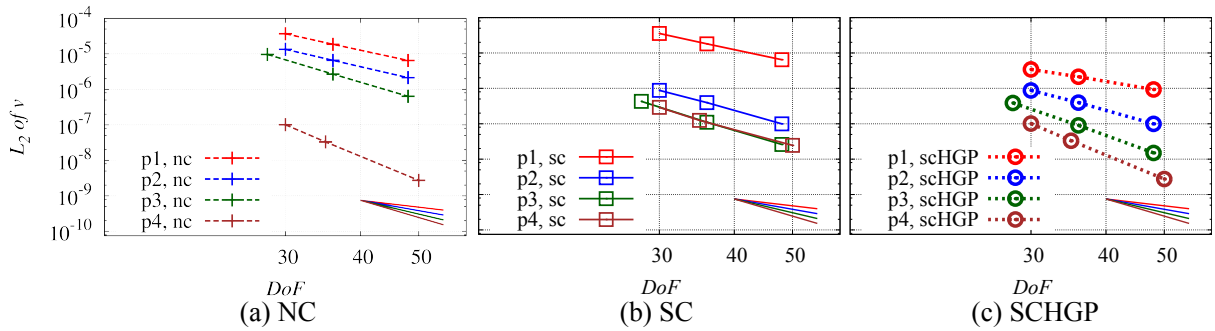

Fig. 4: Order of accuracy of the NC, SC, and SCHGP metrics.

6 Conclusions

We have evaluated the conservative metrics in a high-order conservative FR scheme implemented on a three-dimensional stationary-curvilinear grid with high-order elements. The main findings of this research are summarized below: 1) If both of the SP and correction parts (Eq.(11)) vanish, the reconstructed flux will preserve the freestream. A sufficient condition for global conservation is that the metric values are uniquely determined at each cell boundary; 2) We have proposed SCHGP metric that compatibly satisfies both the freestream preservation and global conservation properties for arbitrary orders of the solution. The SCHGP is constructed such that the order of the metric exactly matches the order of the solution. 3) When SCHGP was applied to metrics, the freestream preservation was attained in the arbitrary order of solution, and the convecting vortex was well preserved with maintaining the formal order of accuracy. On the other hand, when SC (inappropriate implementation of the symmetric conservative metrics) is adopted to the metric, the order of the computational solution is limited by the order of the metric. The proposed technique (SCHGP) is expected to be applicable to the high-order conservative FR scheme with moving and deforming grids although it is beyond the scope of this paper. Finally, when the Radau polynomial is used as a correction function, the freestream preservation error cannot be discussed in the current framework because the SP and correction part will cancel each other in some cases, which is discussd in detail in another paper [14].

Acknowledgments

This research has received contributions from the JSPS Science Research Grant 225879, which we would like to make mention here in expressing our appreciation.

Appendix A Symmetric conservative metrics and surface closure law

We defined the following interpolating polynomials for the symmetric conservative metric (this is equivalent to Eq. (18) or (20)):

$$\hat{\xi}_x^{GP;N} = \partial_\zeta I^{GP;N}[T_A] - \partial_\eta I^{GP;N}[T_B]. \tag{22}$$

When the solution is of K, the SCL identity (9) is computed by:

$$\partial_\xi I^{SP;K}[\hat{\xi}_x^{GP;N}] + \partial_\eta I^{SP;K}[\hat{\eta}_x^{GP;N}] + \partial_\zeta I^{SP;K}[\hat{\zeta}_x^{GP;N}] \tag{23}$$

$$= \underline{\partial_\xi I^{SP;K}[\partial_\zeta I^{GP;N}[T_A]] - \partial_\zeta I^{SP;K}[\partial_\xi I^{GP;N}[T_A]]} + \cdots = 0. \tag{24}$$

We consider the sufficient conditions under which the underlined part of Eq.(24) becomes zero. We rewrite the underlined part of Eq.(24) as follows:

$$\sum_{q=0}^{K}\sum_{j=0}^{N} \phi_q^K(\eta)\phi_j^N(\eta_q) \left[\underbrace{\sum_{r=0}^{K}\sum_{k=0}^{N} \phi_r^K(\zeta) d\phi_k^N(\zeta_r)}_{\text{(ii-a)}} \left\{ \underbrace{\sum_{p=0}^{K}\sum_{i=0}^{N} d\phi_p^K(\xi)\phi_i^N(\xi_p)}_{\text{(i-a)}} T_{A;i,j,k} \right\} \right]$$

$$- \sum_{q=0}^{K}\sum_{j=0}^{N} \phi_q^K(\eta)\phi_j^N(\eta_q) \left[\underbrace{\sum_{r=0}^{K}\sum_{k=0}^{N} d\phi_r^K(\zeta)\phi_k^N(\zeta_r)}_{\text{(ii-b)}} \left\{ \underbrace{\sum_{p=0}^{K}\sum_{i=0}^{N} \phi_p^K(\xi) d\phi_i^N(\xi_p)}_{\text{(i-b)}} T_{A;i,j,k} \right\} \right] \tag{25}$$

Both (i-a)=(i-b) and (ii-a)=(ii-b) are sufficient conditions for reducing Eq.(25) to zero. Differentiation and interpolation become commutative if and only if $K \geq N$. Under this condition, both of (i-a)=(i-b) and (ii-a)=(ii-b) hold. The other underlined terms in Eq.(24) similarly become zero only when $K \geq N$. Therefore, the symmetric conservative metric expressed in the form of Eq.(22) satisfies the SCL identity only when $K \geq N$.

REFERENCES

[1] Huynh, H. T., "A Flux Reconstruction Approach to High-Order Schemes Including Discontinuous Galerkin Methods," *AIAA 2007-4079*, 2007.

[2] Haga, T. and Kawai, S., "Toward Accurate Simulation of Shockwave-Turbulence Interaction on Unstructured Meshes: A Coupling of High- Order FR and LAD Schemes," *AIAA 2013-3065*, 2013.

[3] Kopriva, D., "Metric Identities and the Discontinuous Spectral Element Method on Curvilinear Meshes," *Journal of Scientific Computing*, Vol. 26, 2006, pp. 301–326.

[4] Abe, Y., Iizuka, N., Nonomura, T., and Fujii, K., "Conservative metric evaluation for high-order finite difference schemes with the GCL identities on moving and deforming grids," *Journal of Computational Physics*, Vol. 232, 2013, pp. 14–21.

[5] Abe, Y., Nonomura, T., Iizuka, N., and Fujii, K., "Geometric interpretations and spatial symmetry property of metrics in the conservative form for high-order finite-difference schemes on moving and deforming grids," *Journal of Computational Physics*, Vol. 260, 2014, pp. 163–203.

[6] Thomas, P. D. and Lombard, C. K., "Geometric Conservation Law and its Application to Flow Computations on Moving Grids," *AIAA Journal*, Vol. 17, No. 10, 1979, pp. 1030–1037.

[7] Visbal, M. R. and Gaitonde, D. V., "On the Use of Higher-Order Finite-Difference Schemes on Curvilinear and Deforming Meshes," *Journal of Computational Physics*, Vol. 181, No. 1, 2002, pp. 155–185.

[8] Vinokur, M. and Yee, H., "Extension of Efficient Low Dissipation High Order Schemes for 3-D Curvilinear Moving Grids," *Frontiers of Computational Fluid Dynamics*, 2002, pp. 129–164.

[9] Deng, X., Mao, M., Tu, G., Liu, H., and Zhang, H., "Geometric Conservation Law and Applications to High-Order Finite Difference Schemes with Stationary Grids," *Journal of Computational Physics*, Vol. 230, No. 4, 2011, pp. 1100–1115.

[10] Deng, X., Min, Y., Mao, M., Liu, H., Tu, G., and Zhang, H., "Further studies on Geometric Conservation Law and applications to high-order finite difference schemes with stationary grids," *Journal of Computational Physics*, Vol. 239, 2013, pp. 90–111.

[11] Nonomura, T., Iizuka, N., and Fujii, K., "Freestream and vortex preservation properties of high-order WENO and WCNS on curvilinear grids," *Computers & Fluids*, Vol. 39, No. 2, 2010, pp. 197–214.

[12] Kim, J. W. and Lee, D. J., "Characteristic Interface Conditions for Multiblock High-Order Computation on Singular Structured Grid," *AIAA Journal*, Vol. 41, 2003, pp. 2341–2348.

[13] Kawai, S. and Lele, S., "Localized artificial diffusivity scheme for discontinuity capturing on curvilinear meshes," *Journal of Computational Physics*, Vol. 227, 2008, pp. 9498–9526.

[14] Abe, Y., Haga, T., Nonomura, T., and Fujii, K., "Freestream preservation on a high-order conservative flux-reconstruction scheme," *submitted to Journal of Computational Physics*, 2014.